THE ROBUST DETECTION OF STARS ON CCD IMAGES

FILIP HROCH

Astronomical Institute, Faculty of Science, Masaryk University,
Kotlářská 2, 611 37 Brno, Czech Republic
(e-mail: hroch@physics.muni.cz)

Abstract. Two parameters are developed to analyze the CCD images from ground-based and/or space telescopes. The first parameter, deduced from the intensity profile of the object *sharp*, is useful to resolve stars and hot pixels. The second parameter *shape* distinguishes the stars from the background cosmic-ray events using geometric characteristics defined by its shapes. The parameters are applied to a simulated OMC/INTEGRAL image and a HST image.

Keywords: data analysis, image processing

1. Introduction

The general problem of the fully automatic star detecting algorithms on the CCD images is the successful recognition of real star images or star-like sources in general from other types of objects and defects. These false objects originate from non-ideal characteristics of the CCD instrument (noise, bad column and hot pixels) or from the environment (nebulae, galaxy or cosmic ray events known as 'cosmics'). The frequent requirement is to find real star images on a diffuse background or in a crowded star field. Therefore, the detecting algorithm cannot use a simple intensity comparing principle, because the intensity of non-stellar objects can be comparable to star intensities.

A number of different methods for the automatic star detection on astronomical images has been used during the last two decades. For example, the method based on wavelet transforms applied to satellite ROSAT image processing was published by Damiani *et al*. (1997). The automatic search and classification were implemented in FOCAS routine by Valdes *et al*. (1995). The PC Vista by Trefers and Richmod (1989) is a package for photometry with a simple algorithm for star detection. The well-known program DAOPHOT by Stetson (1987) contains two parameters *sharp* and *round* and a highly robust algorithm for star detection. The determination of these parameters originates from specific characteristics of the sources on CCD images, but both parameters are not sensitive enough to resolve stars and cosmics on the CCD images exposed in focus of a space telescope and/or camera such as the OMC experiment on-board INTEGRAL (Hermsen and Winkler, 1997).

2. Distinguishing Hot Pixels

The large part of the information describing the detected object is included in its intensity profile, but the profile varies widely with weather, telescope focus, etc. changes. The intensity distribution cannot be described by an analytical function, because it depends on many non-controllable factors. Fortunately, the real measured profiles are (in the first approximation) close to the two-dimensional Gaussian profile both for the ground-based (Moffat, 1969) and space telescopes.

From this point of view, we can easy distinguish between the hot pixel (a single pixel with very different intensity compared to surrounding pixels) and the real star. The star image with the Gaussian profile is usually spread over several pixels. For illustration, the typical 1-dimensional profiles of the star and of the hot pixel are shown in Figures 1 and 2. The maximum intensity of the object $I_{i_0 j_0}$ is at the pixel (i_0, j_0). The center of the star is at position

$$x_c = \frac{\sum I_{ij} \cdot i}{\sum I_{ij}} \qquad y_c = \frac{\sum I_{ij} \cdot j}{\sum I_{ij}}, \tag{1}$$

where summations are evaluated over a small area around the central pixel (i_0, j_0) – for example over 5×5 pixels. This notation is also used below. Approximation of the observed intensity by the two-dimensional Gaussian profile is the next step of our algorithm

$$G(i, j) = G_0 e^{-[(i-x_c)^2+(j-y_c)^2]/2h^2} + b \tag{2}$$

The parameter G_0 is the estimated maximum of the star profile, b is the local sky background. The parameter h is the 'width' of the typical star and its numerical value must be known *a priori*. The stars are axis-symmetrical objects according to this formula. Note, that the G_0 parameter is equivalent to, but not quite identical with the Stetson's parameter $H_{i_0 j_0}$ (integer values are used for x_c, y_c, i.e. $x_c \equiv i_0, y_c \equiv j_0$). If we suppose that the statistical distribution of the observed intensity has a normal distribution, we can use the least square method

$$S = \sum (G(i, j) - I_{i,j})^2 \rightarrow \min \tag{3}$$

for the estimation of the unknown G_0 and (further unused) b.

Further, we can estimate the central intensity I_0 from the maximum intensity $I_{i_0 j_0}$ by subtracting the local background intensity $B_{i_0 j_0}$ from $I_{i_0 j_0}$:

$$I_0 = I_{i_0 j_0} - B_{i_0 j_0} \tag{4}$$

where

$$B_{i_0 j_0} = \frac{\sum_{(i,j) \neq (i_0, j_0)} w_{ij} I_{ij}}{\sum_{(i,j) \neq (i_0, j_0)} w_{ij}}$$
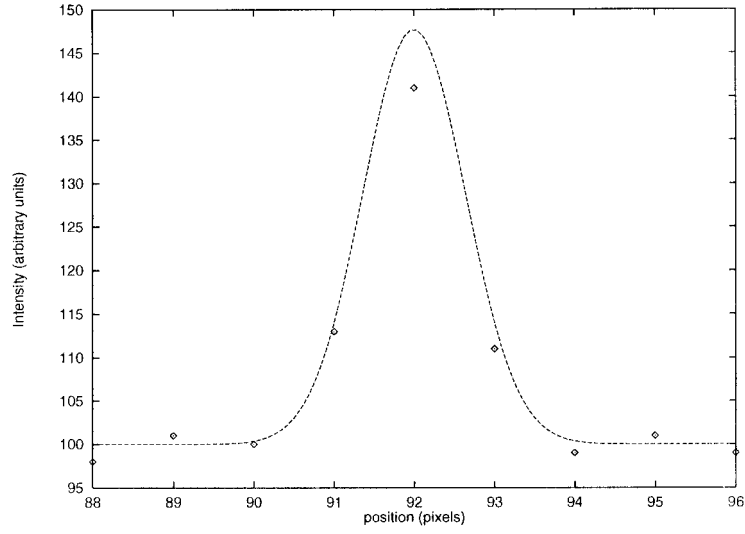
Figure 1. The intensity profile for typical star image. Intensity in arbitrary units, x coordinate in pixels. The Gaussian best fit is plotted with parameters: $G_0 = 50.1$, $h = 0.64$, $x_c = 92.0$, $y_c = 76.8$. The background intensity is 100 and the observed intensity peak $I_0 = 41$ satisfies $G_0 > I_0$.
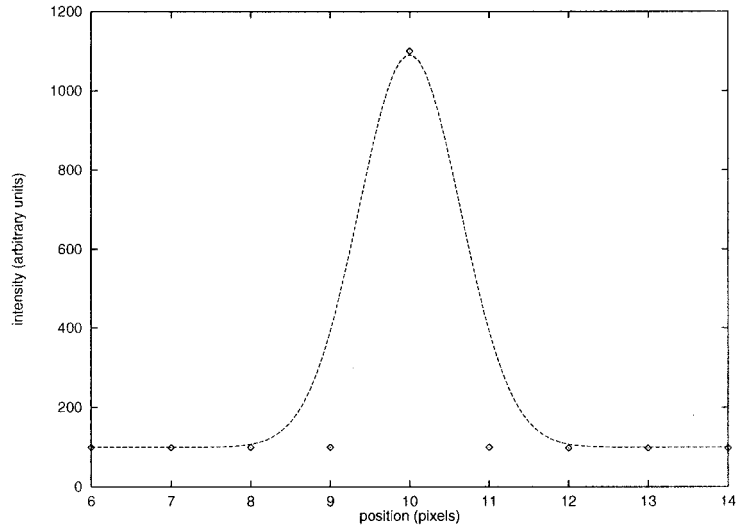

Figure 2. The intensity profile for a hot pixel. Intensity in arbitrary units, x coordinate in pixels. The Gaussian best fit is plotted with parameters: $G_0 = 991.3$, $h = 0.64$, $x_c = 10.0$, $y_c = 90.0$. The background intensity is 100 and the observed intensity peak $I_0 = 1000$ satisfies $G_0 < I_0$.

(w_{ij} are arbitrary weights) and compare its numerical value in parameter *sharp*:

$$sharp \equiv \frac{I_0}{G_0}. \tag{5}$$

The Figures 1 and 2 indicate the typical values of this parameter. Its value is in agreement with the inequality $G_0 > I_0$ for the star and with $G_0 < I_0$ for the hot pixel. We can hence deduce the range of the parameter *sharp* as $0 < sharp < 1$ for the star.

3. Distinguishing Cosmic-Ray Events

The cosmic ray events frequency on the CCD images exposed at a ground-based observatory is low and, moreover, its profiles are narrower than the star profiles. The image processing algorithm can then easily resolve the images of the stars and those of the cosmic-ray events. But CCD images from satellites contain a higher number of the cosmic-ray event tracks and the numerical value of the *sharp* parameter, computed for the stars, is close to the numerical value for cosmics. The construction of the confidentiality test for its distinguishing with only the *sharp* parameter is not possible.

The star isophotes of the ideal images have the shape of concentric circles, but the cosmics or the bad columns are represented in general by ellipses with the major semi-axis at some angle to the x coordinate. The mathematical description of an object in image is derived from this characteristics.

The most effective way is the description of the object by its 2nd moments

$$h_x^2 = \frac{\sum I_{ij}(i - x_c)^2}{\sum I_{ij}}, \qquad h_y^2 = \frac{\sum I_{ij}(j - y_c)^2}{\sum I_{ij}} \tag{6}$$

and

$$h_{xy} = \frac{\sum I_{ij}(i - x_c)(j - y_c)}{\sum I_{ij}} \tag{7}$$

where the summations are evaluated over the same small area around (i_0, j_0). Now, we can compute the lengths of the object semi-axes as the 'eigenvalues' problem. Its lengths satisfy the equation

$$\begin{vmatrix} \lambda - h_x & h_{xy} \\ h_{xy} & \lambda - h_y \end{vmatrix} = 0$$

Resolving of this equations for λ gives the sizes of semi-axes as

$$\lambda_\pm = \frac{1}{2}\left[(h_x + h_y) \pm \sqrt{(h_x - h_y)^2 + 4h_{xy}^2}\right]$$

The numerical values of its parameters (lengths of semi-axes) are different for elongated object, but approximately the same for stars. With respect to their character we define the parameter

$$shape \equiv 2\frac{\sqrt{(h_x - h_y)^2 + 4h_{xy}^2}}{h_x + h_y} \qquad (8)$$

The limits of this parameter are:

− $h_x \to h_y, h_{xy} \to 0 : shape \to 0$, the star case
− $h_x \leftrightarrow h_y, h_{xy} \neq 0 : shape \to 4h_{xy}/(h_x + h_y)$, the cosmics case
− $h_x \neq h_y, h_{xy} \to 0 : |shape| \to 2|(h_x - h_y)/(h_x + h_y)| \gg 0$, the bad column case, *shape* parameter is then equivalent to the *round* parameter of Stetson (1987)

The parameter *shape* describes the shape of the object. The circular objects are interpreted this way as stars and the very elongated object as cosmic-ray events or bad columns. Note, that the *shape* parameter represents direct generalization of the *round* parameter described in Stetson (1987). The *round* parameter is capable of measuring elongation only parallel to rows or columns of the image. It was intended to identify bad rows or columns, not cosmics.

4. The Simulated Image

In this section we describe the use of the parameters mentioned in previous sections to analyze the simulated image of the star field. The image (Figure 3) is generated as the simulation of the field of view of the OMC (Optical Monitoring Camera) prepared for the ESA satellite INTEGRAL. The PSF function of the stars in the image is defined as the two-dimensional Gaussian profile with 70% of the light energy in the central pixel, according to the PSF of the flight optics. This results in $h = 0.64$ for the stars in the simulated image, while their centers are uniformly spread over the unit interval. There are also some other sources in the image, namely the bad column, hot pixels and a few cosmics (Figure 3 and Table I). The image is critically under-sampled.

The image left-bottom corner has coordinates (0, 0) and right-top one (100, 100) in pixels. The bad column is situated at $x_c = 5$. The hot pixels occupy positions (10, 90), (10, 20), (20, 10), (20, 90) and the centers of the three cosmics appear at (10, 10), (40, 10), (62, 15). All other sources represent real stars. The intensity of the sky is 100 with the Gaussian noise 1.1 (all intensities in arbitrary units). Object No. 4 (star) and object No. 1 (hot pixel) were used for construction of the profiles shown in Figures 1 and 2.
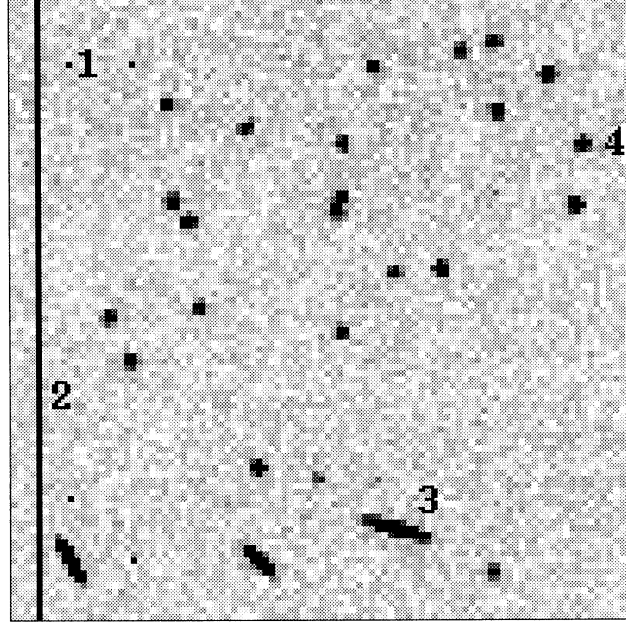
Figure 3. The simulated image with stars and other sources (legend: No. 1 – hot pixel, No. 2 – bad column, No. 3 – cosmics, No. 4 – star).

The computed characteristics for the selected sources in the simulated image are listed in Table I. The center of the object is at coordinates x_c, y_c, see Equation (1), the intensity peak at pixel (i_0, j_0) is related to I_0 according to Equation (4). The moments computed from Equations (6) and (7) are h_x, h_y, h_{xy} and the parameter G_0 is obtained by minimization of the sum (Equation (3)). The last three columns contain the values of the parameters *sharp*, *round* and *shape*.

The values of the numerical differences of the *sharp* parameter for star and hot pixel are small because h is small, but the upper bound at 1 separates stars and hot pixels to obviously different groups. The values of the *round* parameter demonstrate small difference between cosmics and stars. On the contrary the values of the *shape* parameter of the stars (or hot pixels) and of the cosmics as well as that of the bad columns are clearly incompatible.

5. The HST Image

A wide variety of different kinds of objects appears in the simulated image, but the real images can also contain others unpredictable defects. We test the applicability of the parameters on an example of a real image (Figure 4). We have extracted and zoomed a small sub-window of the image from HST. The image has been corrected

TABLE I

The parameters of objects in the simulated image (legend: No. 1 – hot pixel, No. 2 – bad column, No. 3 – cosmics, No. 4 – star)

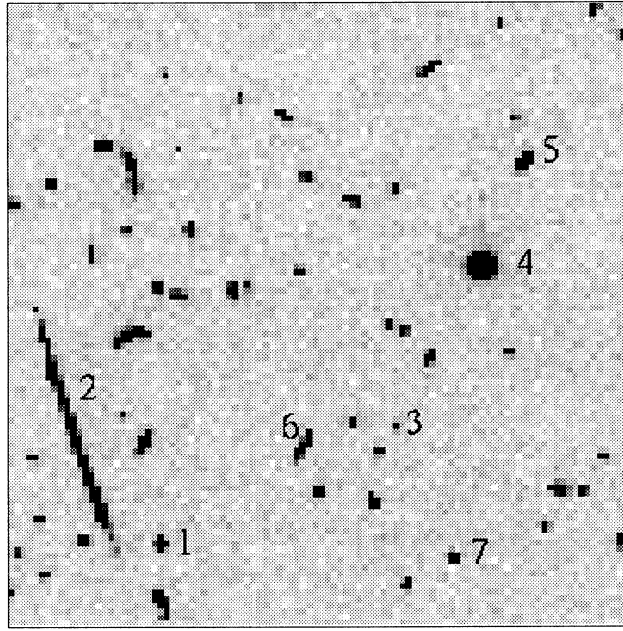| No.	x_c	y_c	I_0	h_x	h_y	h_{xy}	G_0	round	sharp	shape
1	10.0	90.0	1000	0.17	0.17	0.00	991.4	0.02	1.01	0.06
2	5.0	5.0	1000	0.07	1.41	0.00	865.3	–1.81	0.91	1.80
3	62.0	15.0	199	1.30	0.62	–0.46	194.2	0.71	0.92	1.20
4	92.0	76.8	41	0.69	0.66	0.03	50.1	0.04	0.80	0.10

Figure 4. The HST image with stars and cosmics (legend: No. 1 – star, No. 2 – cosmics, No. 3 – star, No. 4 – nebulosity(?), No. 5 – double star, No. 6 – cosmics, No. 7 – star).

on photometric corrections (bias, flat field, etc.) and exhibits no hot pixels or bad columns. We set the value of the *h* parameter to $h = 0.4$.

The list of derived characteristics for a selected objects in this image is given in Table II. The meaning of the columns is identical with Table I. The objects numbers correspond with Figure 4. The intensity of the sky is 8.3 with the Gaussian noise 1.5 (all in arbitrary units).

Identifying by 'a visual method' leads to classify the objects No. 1, 3 and 7 as stars, No. 2 and 6 as cosmics, No. 4 as nebulosity and No. 5 is probably a double star. The values of the *sharp* parameters are in the range valid for stars (and

TABLE II

The parameters of objects in the HST image (legend: No. 1 – star, No. 2 –cosmics, No. 3 – star, No. 4 – nebulosity(?), No. 5 – double star, No. 6 – cosmics, No. 7 – star)

No.	x_c	y_c	I_0	h_x	h_y	h_{xy}	G_0	round	sharp	shape
1	25.0	13.8	406.00	0.33	0.54	0.00	774.39	–0.49	0.51	0.49
2	9.0	38.0	724.00	0.41	0.95	–0.26	717.75	–0.79	0.96	1.11
3	63.1	33.0	90.00	0.60	0.60	–0.01	116.62	0.00	0.70	0.04
4	77.1	59.1	419.00	0.97	0.98	0.02	502.82	–0.01	0.77	0.04
5	83.8	75.9	450.00	0.63	0.76	0.31	723.16	–0.19	0.59	0.92
6	48.3	30.2	124.00	0.74	1.24	0.72	877.73	–0.51	0.12	1.54
7	72.3	11.9	307.00	0.53	0.38	0.00	1447.14	0.32	0.20	0.32

hence indicating the absence of hot pixels). 'The visual method' classification of stars and cosmics confirms the values of the *shape* parameter – values for cosmics significantly exceeds 1. The *round* parameter has little use for successful recognition between stars and cosmics. This example can be described as a typical one, because the stars, galaxies and cosmics represent the most frequent objects in the HST images. The double star case (No. 5) complicates this test and it can easily result in the failure of the whole procedure – the *shape* parameter can be near the limit set in the algorithm boundary threshold and we have to set it carefully.

6. Conclusions

The two parameters *sharp* and *shape* described in this paper are widely applicable to the robust detection of the star-like sources in images provided by array detectors. The primary reason for deriving the parameters was the development of a reliable automatic algorithm for the recognition of stars on CCD images. We can choose following criterion for this purpose it the intensity of the central pixel of the examined object is above an arbitrarily defined 'level of significance' (threshold) and the object lying far from the edge of the frame. Then

(a) the object is a star for: $0 < sharp < 1$ and $0 < shape < 1$.
(b) the object is a cosmics for: $shape > 1$.
(c) the object is a bad column for: $shape > 1$.
(d) the object is a hot pixel for: $sharp > 1$.

This definition provides a strict mathematical criterion for detection and classification of the various kinds of objects on CCD images.

We might specify a range of the *sharp* and *shape* parameters for a star centered on a pixel as $0 < sharp < 1$, $0 < shape < 1$. The range of *sharp* for a star centered on the edge between two pixels decrease to $0 < sharp < 1/2$ and one for a star centered on the corner of four pixels decrease to $0 < sharp < 1/4$, but the range for *shape* increase to $0 < shape < 2$ in this both cases.

Acknowledgements

References

Damiani, F. A. *et al*.: 1997, *Astrophys. Journal* **483**, 350.
Hermsen, W. and Winkler, C.: 1997, Proc. IAU Symposium, 188.
Moffat, A. F. J.: 1969, *Astronomy and Astrophysics* **3**, 455.
Stetson, P. B.: 1987, *Publ. ASP* **99**, 191.
Treffers, R. and Richmond, M.: 1989, *Publ. ASP* **101**, 725.
Valdes, F. G. *et al*.: 1995, *Publ. ASP* **107**, 1119.